

Low-Dosage Ozonation in Gaseous VOCs Biofilter Promotes Community Diversity and Robustness

Marvin Yeung

Tsinghua University School of Environment

Prakit Saingam

University of Hawai'i at Manoa Department of Civil and Environmental Engineering

Yang Xu

Tsinghua University School of Environment

Jinying Xi (✉ xijinying@tsinghua.edu.cn)

Tsinghua University School of Environment <https://orcid.org/0000-0002-1734-8973>

Research

Keywords: Microbial community diversity, metabolic rates of different carbon sources

Posted Date: August 19th, 2020

DOI: <https://doi.org/10.21203/rs.3.rs-58642/v1>

License: © ⓘ This work is licensed under a Creative Commons Attribution 4.0 International License.

[Read Full License](#)

Version of Record: A version of this preprint was published on January 12th, 2021. See the published version at <https://doi.org/10.1186/s40168-020-00944-4>.

Abstract

Background

Ozonation of biofilter is known for alleviating clogging and pressure drop issues while maintaining removal performances in biofiltration systems treating gaseous VOCs (Volatile Organic Compounds). The implications of ozone on the biofilter microbiome, in terms of biodiversity, community structure, metabolic abilities and dominant taxa correlated with performance remain largely unknown.

Methods

This study investigated two biofilter treating high concentration toluene operating in parallel, with one acting as control and the other exposed to low-dosage (200 mg/m³) ozonation. Microbial community diversity, metabolic rates of different carbon sources, functional predictions and microbial co-occurrence networks of both communities were examined.

Results

Consistently higher biodiversity of over 30% was observed with microbiome after ozonation, with increased overall metabolic abilities for amino acids and carboxylic acids. Relative abundance of species with reported stress tolerant and biofilm forming abilities significantly increased, with a consortium of changes in predicted biological pathways, including shifts in degradation pathways of intermediate compounds, while correlation of top OTUs and genus with performance indicators show diversifications in microbiota responsible for VOCs degradation. Co-occurrence network of the community shows a decrease in average path distance and average betweenness with ozonation.

Conclusion

Shifts in major degrading species and increase in biodiversity could explain the consistent performance commonly seen in ozonation of biofilters despite the decrease in biomass. Increased presence of stress tolerant microbes in the microbiome coupled with decentralization of the co-occurrence network suggest that ozonation could not only provide amelioration for clogging issues but also provides a microbiome more robust to loading shocks seen in full-scale biofilters.

1. Introduction

Biofiltration is a technology widely applied in abatement of VOCs emissions, known for its low cost (Jorio et al., 1998; Metris et al., 2001; Strauss et al., 2004) and minimal secondary pollution (Iranpour et al., 2005; Deng et al., 2012). A persisting issue present in applications of biofilters is the excessive growth of biomass, resulting in clogging, increased pressure drop and decreased removal performances (Alonso et al., 1997; Okkerse et al., 1999). Various biomass control methods were developed to solve clogging issues (Yang et al., 2010). One technique of ozone injection was previously reported (Xi et al., 2014), complemented by another study examining the metabolic activities of microbiome in biofilter under O₃

exposure, concluding an increase in metabolism rate of numerous carbon sources of lower biodegradability, such as γ -hydroxybutyric acid, d-galactonic acid γ -lactone, d-mannitol, d-cellobiose and γ -methyl-d-glucoside etc. (Saingam et al., 2016). Traditionally O_3 is regarded as a strong oxidant that purges microorganisms and lowering overall activity. However, the opposite response was found in low-dosage O_3 exposure. For example, low concentration O_3 (e.g. 120 mg m⁻³) was found to improve metabolic activity (Wang et al., 2009). It was shown that despite the decrease in biomass, microbial activity for metabolism of multiple carbon sources increased in the biofilter, implying an inherent change in the microbial level. It is well known that the microbiome of a biofilter is crucial for effective pollutant abatement (Ralebitso-Senior et al., 2012), yet the exact microbiome and functional changes that occur allowing increased microbial activity while maintaining system performance with decrease in biomass remained intriguing and unknown. In this study, 16srRNA sequences of the v4 region in a controlled biofilter and ozonated biofilter operated in parallel was sequenced for investigation of microbial changes leading to the adaptation and performance changes of the microbiome. Using statistical analysis techniques, we attempt to explicate the relevance of dominant taxa treating toluene after addition of O_3 , using latest databases we predict changes in functional and phenotypic characteristics under ozonation, and quantifying relations of microbiome change with removal performances.

2. Methodology

2.1 Experimental setup

Two lab-scale biofilters named BF1 and BF2, constructed as acrylic cylinder with 12 cm inner diameter and 25 cm height. Each biofilter was packed with porous perlite (0.54 void fraction) to form a 1.6 L filter bed 15.0 cm in height. An air compressor (Hailea ACO-318, Fuzhou, China) was used to feed air into the system. Toluene gas inlet was produced with fresh air passing through a bottle containing liquid toluene. The gas flow rate was controlled by a flow meter (Zenxing LZD-4WB, Xianghu, China). A stainless-steel reactor equipped with a UV lamp (Cnlight ZW23D15W-Z436, Shenyang, China) was used to generate gaseous ozone for BF1. For each biofilter, the packing media was initially mixed with 1.0 L activated sludge collected from a municipal wastewater treatment plant (Xiaojiahe WWTP, Beijing, China). Nutrient solution containing $NaNO_3$ (20 g/L), Na_2HPO_4 (1.6 g/L) and KH_2PO_4 (1.04 g/L) was sprayed directly on filter beds of the two biofilters for sufficient humidity and nutrients. The leachate was discharged every day. The two biofilters were operated in parallel for 160 days in total, both operated in identical conditions without ozone for the first 44 days, BF1 was fed with 200 mg/m³ gaseous ozone after day 45.

2.2 Microbial sampling

Microbial samples were taken from both biofilters at day 66, 80, 94 and 160, packing media were taken from depths of 1 cm, 7 cm, 15 cm of the filter bed, biofilms were detached and suspended in phosphate buffer saline (PBS) by sonication at 425 W, 21–25 kHz for 10 min (Ningbo Science Biotechnology SCIENTZ-IID, Ningbo, China). The sonicated suspension was centrifuged at 10000 × g for 1 min and resuspended in 5 ml PBS. To exclude dead cells within the community, a fluorescent dye (propidium

monoazide, PMA) was used to treat the microbial suspension by inactivating DNA of cells of damaged cell membrane as well as exposed DNA (Guo and Zhang, 2014). PMA (Biotum, PMA™ dye, USA) stock was prepared by dissolving 1 mg PMA in 100 µL of 20% dimethyl sulfoxide (DMSO) and stored at - 20 °C; 2.5 µL 20 mmol/L PMA solution was added into 500 µL microbial suspension. The mixture was incubated at room temperature for 5 min and occasionally mixed. The tubes were placed horizontally on ice and exposed to a 650 W halogen light, at 20 cm distance, for 4 min. Then, DNA from PMA-treated aliquot are isolated with the FastDNA® SPIN Kit for Soil (MP Biomedicals, USA) following the manufacturer's instruction.

Each sample from a particular biofilter at a particular time were divided into 3 identical samples after PMA treatment and before DNA extraction, therefore each sample was represented as triplets to counter systematic biases from DNA isolation and sequencing procedures.

2.3 High-throughput sequencing and data analysis

The PCR reaction was performed with the following cycling conditions: 95 °C for 3 min, followed by 30 cycles of 98 °C for 20 sec, 55 °C for 15 sec, and 72 °C for 15 sec, with a final extension of 72 °C for 1 min. Sequencing of the 16 s rDNA V4 region was carried out on an Illumina Miseq platform. The primer 515F (5'-GTGCCAGCMGCCGCGTAA-3') and the sequence of reverse primer 806R (5'-GGACTACHVGGGTWTCTAAT-3') was used. Barcodes and adapter sequences were trimmed with Cutadapt (Martin, 2011), later truncated at 200 bp and denoised with DADA2 to formulate the ASV(Amplicon sequence variants) table (Callahan et al., 2016). Taxonomy of 16srRNA sequences were classified with the Greengene 13.8 16 s rRNA database at 99% similarity with Naïve-Bayes algorithm (Desantis et al., 2006; Glick, et al., 2004). Function predictions were done with softwares Bugbase and PICRUSt2 (version 2.1.2b) (Ward et al., 2017; Douglas et al., 2020). Statistical analysis including alpha and beta analysis were conducted in the R package Phyloseq (version 1.3) (McMurdie et al., 2013), R package ALDEx2 (version 1.2) was used to statistically identify pathways highly specific to ozone and control biofilters (Fernandes, Reid et al. 2014). Correlation analysis were performed and plotted using pearson correlation incorporated in the R package ggcor (Huang et al., 2020). Co-occurrence network analysis were conducted with the Molecular ecological network analyses with spearman correlation, Bray-Curtis dissimilarity, RMT (Random matrix theory) threshold of 0.81 (Deng et al., 2012). Networks were plotted with Java software Gephi (Bestian et al., 2009). All R packages were conducted under R version 3.6.

2.4 Metabolic activity analysis

Suspension from sonification containing detached microbiome from the packing media as described in part 2.2 is diluted in PBS to obtain optical density at 600 nm wavelength (O.D.₆₀₀) at 0.05. Then, the ECO plate (Biolog, Inc, USA), with 31 various sources of carbon substrates mixed with the tetrazolium dye, was prepared for the determination. 150 µL of the microbial dilutions was inoculated to each well of the ECO plate and incubated at 30 °C. The plate was observed for the absorbance at 600 nm regularly during 3 days period by the microplate reader (Molecular devices, Spectramax M5, USA). Absorbance over time

from wells of containing carbon source of a same group (e.g. amino acid) is averaged and deducted with the absorbance from the control well to avoid systematic error, and obtaining average metabolic rates of different groups of carbon sources.

3. Results

3.1 Sequencing results

10,000–25,000 sequences of 250 bp were obtained, samples with under 13,000 sequences were discarded and others are rarefied at 13,000 sequences, resulting in 24 samples. 3296 OTUs were identified after denoising.

3.2 System performance

Effects of O₃ on performance data during the period was reported in detail in a previous publication (Saingam et al. 2017), both biofilters had approximately 65% – 70% removal rate treating inlet toluene ranging from 500 to 1500 mg/m³, with no significant difference under t-test (p = 0.62).

3.3 Biodiversity

Biodiversity index comparing the two biofilters are shown in Fig. 1. Intra-group diversity spanned over 400 in both groups of observed diversity, but median and average diversity of ozone biofilter is consistently higher than those of the control samples, indicating an increase in phylogenetic diversity range and average evenness.

3.4 Community differences and propensity of variables

Clear separation of microbiome composition is seen between the two biofilters, whereas intra-group differences also fluctuated considerably with time, relative abundance of major phyla *Actinobacteria*, *Proteobacteria*, *Firmicutes*, *Bacteroidetes* and *TM7* were added as constraining variable in Fig. 2b to show overall compositional difference of OTUs level and abundance differences of major phyla. In addition to prediction of microbiome functions, microbiome phenotypic metabolizing activity from Biolog ECO plates were adopted as constraining variable to show inclination of communities for different carbon sources in Fig. 2b. *Proteobacteria* remained dominant in relative abundance, ozone stimulated its presence despite it consisting mostly of gram-negative species, along with *Firmicutes*, consisting mostly of gram-positive species. *Actinobacteria* is another known gram-positive bacteria seen in biofilters, decreased with ozonation. Metabolization ability of groups of amino acids and carboxylic acids increased in microbiome under ozonation, each containing a consortium of numerous compounds from the groups, while metabolization rates for complex carbohydrates decreased, metabolization data of individual compounds are provided in supplementary material 1.

3.5 Functional characteristics and traits caused by ozonation

Phenotypic traits of microbiome from both biofilters are shown in Fig. 3. In contrast of the

greater intra-group differences seen in biodiversity and OTU level community differences, results of functional traits are relatively clustered, with expected increases in microbes capable of mobility, biofilm formation and stress tolerance with induction of ozonation, yet median proportion of gram-positive strains dropped from 42–27% after ozonation, in contrast with common understandings.

Metacyc pathways predicted by PICRUSt2 that changed substantially with an ALDEx effect size of over 2.5 is shown in Fig. 4. Among 15 pathways highly specific to ozonation, mycolate biosynthesis, taxadiene biosynthesis (engineered), superpathway of heme biosynthesis from glycine, (5Z)-dodec-5-enoate biosynthesis are crucial pathways for assembling of proteins for cell membrane synthesis, although gram-negative bacteria increased with ozonation, repair and synthesis of cell membrane to mitigate oxidative disruption of ozone is seen in microbiome, along with production of anti-oxidants such as heme production and UDP-glucose-derived O-antigen biosynthesis. Of all enriched pathways after ozonation, phenylacetate degradation I (aerobic) pathway is the most significant with effect size of over 2.5, phenylacetate and degradation of other compounds containing acetate groups are widely seen in essential steps of toluene and xylene degradation, both recalcitrant compounds commonly seen as VOCs pollutants (Vardar et al. 2004, Leutwein et al. 2001). Purine ribonucleosides degradation feeding the urea cycle and aspartate degradation and pyrimidine deoxyribonucleosides degradation all contributes to degradation of amino acids, though not directly fed to the microbiome, could be enriched. with the continuous death and accelerated cycle of cells under ozonation, contributing to the increased ability for utilization of amino acids shown in phenotypic metabolization results.

Decrease in TCA cycle participation is seen in ozonation filter, and pathways for degradation of other metabolites in VOCs degrading pathways such as 3-phenylpropanoate and inositol degradation is seen, indicating a motley ununiform changes in pathways after ozonation, no decisive changes affecting overall functional ability are seen between groups, but a mixture of degradation inclination changes favoring different parts of the VOCs degradation pathways.

3.6 Correlation of system performance and dominant taxa

Due to high redundancy known to bacterial populations (Escalas, Hale et al. 2019), majority of function is commonly assumed to be performed by the most abundant taxa in certain microbiome. Dominant taxa of both OTU and Genus level with top 20 relative abundance is selected and their abundance in different samples and operation time were plotted with removal efficiency and mineralization rates of corresponding samples, to investigate difference and similarity of reaction of dominant taxa and their relationship with performance measures, as shown in Fig. 5. By comparing both removal efficiency and mineralization rate, insights can be drawn from removal of toluene and complete degradation to CO₂ and hence intermediate metabolites.

Both correlation of OTU and Genus level are chosen to investigate possible intra-genus differentiation and radicality of differences. 9 out of 20 genera are monotonously correlated with removal efficiency in

both ozone and control biofilter, whereas only 3 out of 20 OTUs are monotonously correlated with removal efficiency, indicating a high specificity and different reaction of OTUs under same genus towards ozonation. genus *Rhodococcus* was reported in numerous studies to be dominant in degradation of xenobiotics in biofilter systems (Portune, Perez et al. 2015, Allievi, Silveira et al. 2018), all four OTUs from the genus *Rhodococcus* present in this system are strongly proportional with removal efficiency in control biofilter but all negatively correlates in ozonated biofilter, suggesting a shift of degrading contribution by *Rhodococcus* and more towards OTUs of genera *Devosia*, *Aquamicrobium* and *Rhizobiales* with high positive correlation with performance, similar trends of these three genus are seen in combined genus level.

3.7 Topological analysis and co-occurrence network construction of microbiome

91 and 107 nodes, 146 and 256 links, 5.1 and 3.6 average path distance were found for control and ozone biofilters respectively, with the increase of average degree from 3.2 to 4.7 under identical specifications for network construction. A more connected and even network is seen in ozone microbiome, smaller path distance coupled with smaller centralization of betweenness is commonly seen as higher stability as major hubs are more diverged and less nodes are likely to be affected under shocks. Major hubs in control biofilter such as OTU68 and OTU309 are substantially irrelevant in ozone biofilter, indicating a radical change in microbial network and hub distribution, yet OTU26 corresponding to the genus *Pandoreae* remain highly relevant in betweenness and degree count in both system, genus *Pandoreae* was reported to be highly enriched in species capable of effective degradation of xenobiotics (Peeters, De Canck et al. 2019), and is positively correlated with $r > 0.7$ in both biofilters in as shown in Fig. 6. Exact OTU taxonomy can be seen in supplementary material 2.

4. Discussion

The performance of pollutant removal is the main concern for improvements attempts on alleviating clogging issues, ozonation was reported in numerous studies to improve or maintain VOCs removal performance while significantly reducing biomass growth rates (Xi et al., 2015, Maldonado-Diaz and Arriaga, 301 2015; Wang et al., 2009). Results from our study for a period of 160 days is consistent with previous studies that no statically significant changes were seen in terms of removal efficiency treating at a relative higher loading rate (fluctuating between 20–70 mg/L/h) compared to usual full-scale applications, showing to be a suitable candidate for full-scale application with the ease of retrofitting and flexible manipulation as ozone can be simply mixed with the inlet gas flow. Oxidative stress such as ozonation is known to reduce diversity at higher dosage, but our results show the opposite, possibly due to a low-enough dosage to allow subsistence of strains more sensitive to oxidative stress while also stimulating the ones more robust, hence providing a more diverse microbiome. Given the diverse nature of xenobiotics degradation pathways, and the complexity of pollutant composition frequently seen in full-scale application, ozonation provided possibility as a method for steady stimulation of microbiome diversity, which was reported to correlate directly with community stability and resistance to shocks

(Hillebrand et al., 2008), which are most commonly seen as spikes in loading rates during periods spanning from hours to months in full-scale operation depending on the particular scenario (Yang et al., 2008). Microbial co-occurrence network shown in Fig. 6 also support this hypothesis with a more decentralized microbiome network after ozone dosage that may be less likely to see changes in community structure as radical as it would be in centralized network of the control biofilter microbiome.

After ozonation, *Proteobacteria* increased in relative abundance, which was widely reported to contain dominant degrader of xenobiotics in both biofilter and wastewater treatments (Allievi, Silveira et al. 2018, Van der Heyden, De Mulder et al. 2019), reported for higher presence in treatment of more complex pollutant and higher loading stress, inducing higher functional diversity (Friedrich and Lipski 2010). In contrast, this could be a phenotypic embodiment of larger community diversity seen in sequencing results, the ability to better metabolize carbon sources other than the only provided toluene, while degradation of xenobiotics such as toluene had highly diverse prokaryotic pathways, a more even and less specialized phenotypic functional profile may be desirable in full-scale applications when composition of pollutants is largely fluctuated, though this decrease of complex carbohydrate degradation and increases in other compounds caused by ozonation did not impinge removal efficiency of biofilter.

Increase in stress tolerance of microbiome is highly desirable in biofilters as common applications of biofilters include emission of periodic fermentation, and highly diverse pollutant seen in chemical engineering industries and pharmaceutical industries depending on the production agenda. Such variations in inlet introduce shocks and hinder performances of biofilter by eliminating degrading strains unfit for the new environment (Cabrol and Malhautier 2011), with the consistently increased stress tolerant strains after ozonation while maintain performance, such shocks in full-scale situations could be mitigated to an extent and is highly desirable. Increase in the biofilm forming population could be an issue in traditional biofilters with clogging issues mentioned above, but ozonation of biofilters was shown to greatly reduce growth rate of overall biomass and elevating pressure drop, the increase in biofilm formation population can hence be considered uncorrelated for steady operation of biofilters after inoculation phase.

Ozonation of biofilter has proven to alleviate clogging issues while maintaining performance, this study revealed other potential improvements to the microbiome such as higher biodiversity and functional stability, attested by a more connected and robust topological network with less centralized distribution and lower average path, a higher percentage of microbiome being stress tolerant while phenotypically achieving higher metabolization rate for a variety of carbon sources, all contribute to shaping a more robust and shock-resistant microbiome. Improvements of the microbiome is another positive aspect of ozone application along with ease of retrofitting and solving clogging issues in full-scale application.

Conclusion

Shifts in major degrading species corresponding to performance and increase in community biodiversity could explain the consistent performance commonly seen in ozonation of biofilters despite the decrease in biomass. Increased presence of stress tolerant microbes in the microbiome coupled with decentralization of the co-occurrence network suggest that ozonation could not only provide amelioration for clogging issues but also provides a microbiome more robust to loading shocks seen in full-scale biofilters.

Declarations

Availability of data and materials: Sequence data of all samples are available at: GenBank BioProject accession number PRJNA656689. Codes used for statistical analysis and plotting can be accessed at: <https://github.com/myhyeung/Low-Dose-Ozonation-in-Gaseous-VOCs-Biofilter-Promotes-Community-Diversity-and-Robustness>.

Funding: This study was supported by the National Natural Science Foundation of China (No.51378286), and the State Environmental Protection Key Laboratory of Microorganism Application and Risk Control.

Conflicts of Interest: The authors declare no conflict of interest.

Ethics approval and consent to participate: Not applicable

Consent for publication: Not applicable

Competing interests: The authors declare that they have no competing interests

Authors' contributions: MY performed analysis of the data and was the sole contributor in writing the manuscript. PS performed the operation and experiments of the biofilters and sampling. XY provided guidance and help during operation and sampling. JX is the corresponding author and provided funding, guidance, facilities for this study.

Acknowledgements: We thank Dr. Dao Guohua for his help on this project.

References

1. Auffret M, Labbé D, Thouand G, Greer CW, Fayolle-Guichard F. Degradation of a mixture of hydrocarbons, gasoline, and diesel oil additives by *Rhodococcus aetherivorans* and *Rhodococcus wratislaviensis*. *Appl Environ Microbiol*. 2009;75(24):7774–82.
2. Yang C, Chen H, Zeng G, Yu, Guanlong, Luo, Shenglian. Biomass accumulation and control strategies in gas biofiltration. *Biotechnology advances*. 2010;28:531–40. 10.1016/j.biotechadv.2010.04.002.
3. Berenjian A, Chan N, Malmiri HJ. Volatile organic compounds removal methods: a review. *Am J Biochem Biotechnol*. 2012;8(4):220–9.

4. Cape JN. Effects of airborne volatile organic compounds on plants. *Environ Pollut.* 2003;122(1):145–57.
5. Cox HH, Deshusses MA. Biomass control in waste air biotrickling filters by protozoan predation. *Biotechnol Bioeng.* 1999;62(2):216–24.
6. Delhoménie MC, Bibeau L, Gendron J, Brzezinski R, Heitz M. A study of clogging in a biofilter treating toluene vapors. *Chem Eng J.* 2003;94(3):211–22.
7. Dorado AD, Baeza JA, Lafuente J, Gabriel D, Gamisans X. Biomass accumulation in a biofilter treating toluene at high loads–Part 1: Experimental performance from inoculation to clogging. *Chem Eng J.* 2012;209:661–9.
8. Dosti B, Guzel-Seydim, ZE.Y.N.EP, Greene AK. Effectiveness of ozone, heat and chlorine for destroying common food spoilage bacteria in synthetic media and biofilms. *Int J Dairy Technol.* 2005;58(1):19–24.
9. Caspi, et al. "The MetaCyc database of metabolic pathways and enzymes". *Nucleic Acids Res.* 2018;46(D1):D633–9.
10. Allievi MJ, Silveira DD, Cantao ME, Filho PB. "Bacterial community diversity in a full scale biofilter treating wastewater odor.". *Water Sci Technol.* 2018;77(7–8):2014–22.
11. Cabrol L, Malhautier L. "Integrating microbial ecology in bioprocess understanding: the case of gas biofiltration.". *Appl Microbiol Biotechnol.* 2011;90(3):837–49.
12. Escalas A, Hale L, Voordeckers JW, Yang Y, Firestone MK, Alvarez-Cohen L, Zhou J. "Microbial functional diversity: From concepts to applications.". *Ecol Evol.* 2019;9(20):12000–16.
13. Fernandes AD, Reid JN, Macklaim JM, McMurrough TA, Edgell DR, Gloor GB. "Unifying the analysis of high-throughput sequencing datasets: characterizing RNA-seq, 16S rRNA gene sequencing and selective growth experiments by compositional data analysis. " *Microbiome.* 2014;2:15.
14. Friedrich MM, Lipski A. "Characterisation of hexane-degrading microorganisms in a biofilter by stable isotope-based fatty acid analysis, FISH and cultivation.". *Appl Microbiol Biotechnol.* 2010;85(4):1189–99.
15. Peeters C, De Canck E, Cnockaert M, De Brandt E, Snauwaert C, Verheyde B, Depoorter E, Spilker T, LiPuma JJ, Vandamme P. "Comparative Genomics of *Pandoraea*, a Genus Enriched in Xenobiotic Biodegradation and Metabolism.". *Front Microbiol.* 2019;10:2556.
16. Portune KJ, Perez MC, Alvarez-Hornos FJ, Gabaldon C. "Investigating bacterial populations in styrene-degrading biofilters by 16S rDNA tag pyrosequencing.". *Appl Microbiol Biotechnol.* 2015;99(1):3–18.
17. Van der Heyden C, De Mulder T, Volcke EIP, Demeyer P, Heyndrickx M, Rasschaert G. Long-term microbial community dynamics at two full-scale biotrickling filters treating pig house exhaust air. *Microb Biotechnol.* 2019;12(4):775–86.
18. Bolyen E, Rideout JR, Dillon MR, Bokulich NA, Abnet CC, Al-Ghalith GA, ... Bai Y. Reproducible, interactive, scalable and extensible microbiome data science using QIIME 2. *Nature biotechnology.* 2019;37:852–7.

19. Callahan BJ, Mcmurdie PJ, Rosen MJ, Han AW, Johnson AJA, Holmes SP. Dada2: high-resolution sample inference from illumina amplicon data. *Nat Methods*. 2016;13:581–3.
20. Louca S, Parfrey LW, Doebeli M. Decoupling function and taxonomy in the global ocean microbiome. *Science*. 2016;353:1272–7.
21. Martin M. Cutadapt removes adapter sequences from high-throughput sequencing reads. *EMBnet journal*. 2011;17:10–2.
22. Rognes T, Flouri T, Nichols B, Quince C, Mahé F. VSEARCH: a versatile open source tool for metagenomics. *Peer J*. 2016;4:e2584.
23. Glick M, Klon AE, Acklin P, Davies JW. Enrichment of extremely noisy high-throughput screening data using a naive Bayes classifier. *J BioMol Screen*. 2004;9:32–6.
24. DeSantis TZ, Hugenholtz P, Larsen N, Rojas M, Brodie EL, Keller K, Huber T, Dalevi D, Hu P, Andersen GL. Greengenes, a Chimera-Checked 16S rRNA Gene Database and Workbench Compatible with ARB. *Appl Environ Microbiol*. 2006;72(7):5069–72. DOI:10.1128/AEM.03006-05.
25. Quast C, Pruesse E, Yilmaz P, et al. The SILVA ribosomal RNA gene database project: improved data processing and web-based tools. *Nucleic Acids Res*. 2013;41(Database issue):D590–6. doi:10.1093/nar/gks1219.
26. Ralebitso-Senior T, Komang, Senior E, Di Felice R, Jarvis K. (2012). Waste Gas Biofiltration: Advances and Limitations of Current Approaches in Microbiology. *Environmental science & technology*. 46. 8542–73. 10.1021/es203906c.
27. phyloseq: An R Package for Reproducible Interactive Analysis and Graphics of Microbiome Census Data
McMurdie PJ, Holmes. 2013. phyloseq: An R Package for Reproducible Interactive Analysis and Graphics of Microbiome Census Data. phyloseq: An R Package for Reproducible Interactive Analysis and Graphics of Microbiome Census Data.
28. PLOS ONE. 8(4): e61217. <https://doi.org/10.1371/journal.pone.0061217>.
29. Tonya Ward J, Larson J, Meulemans B, Hillmann J, Lynch D, Sidiropoulos JohnR, Spear. Greg Caporaso, Ran Blekhman, Rob Knight, Ryan Fink, Dan Knights. BugBase predicts organism-level microbiome phenotypes. doi: <https://doi.org/10.1101/133462>.
30. Nhu H, Nguyen Z, Song ST, Bates S, Branco L, Tedersoo J, Menke JS, Schilling PG, Kennedy. FUNGuild: An open annotation tool for parsing fungal community datasets by ecological guild, *Fungal Ecology*, Volume 20, 2016, Pages 241–248, ISSN 1754–5048, <https://doi.org/10.1016/j.funeco.2015.06.006>.
31. Wemheuer F, Taylor JA, Daniel R, et al. Tax4Fun2: prediction of habitat-specific functional profiles and functional redundancy based on 16S rRNA gene sequences. *Environmental Microbiome*. 2020;15:11. <https://doi.org/10.1186/s40793-020-00358-7>.
32. Huang H, Zhou L, Chen J, Wei T. (2020). ggcor: Extended tools for correlation analysis and visualization. R package version 0.9.7.

33. Deng Y, Jiang Y, Yang Y, et al. Molecular ecological network analyses. *BMC Bioinformatics*. 2012;13:113. <https://doi.org/10.1186/1471-2105-13-113>.
34. Bastian M, Heymann S, Jacomy M. (2009). Gephi: an open source software for exploring and manipulating networks. *International AAAI Conference on Weblogs and Social Media*.
35. Hillebrand H, Bennett DM, Cadotte MW. Consequences of dominance: a review of evenness effects on local and regional ecosystem processes. *Ecology*. 2008;89:1510–20.
36. Yang LH, Bastow JL, Spence KO, Wright AN. What can we learn from resource pulses. *Ecology*. 2008;89:621–34.

Figures

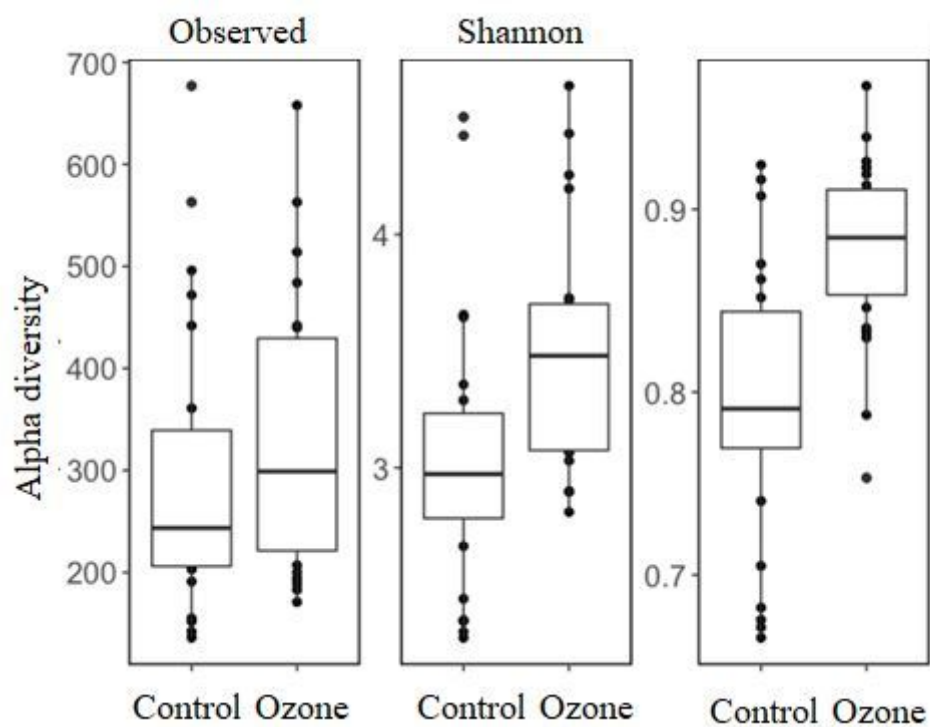


Figure 1

Observed, Shannon and Simpson diversity index of samples of the two biofilters.

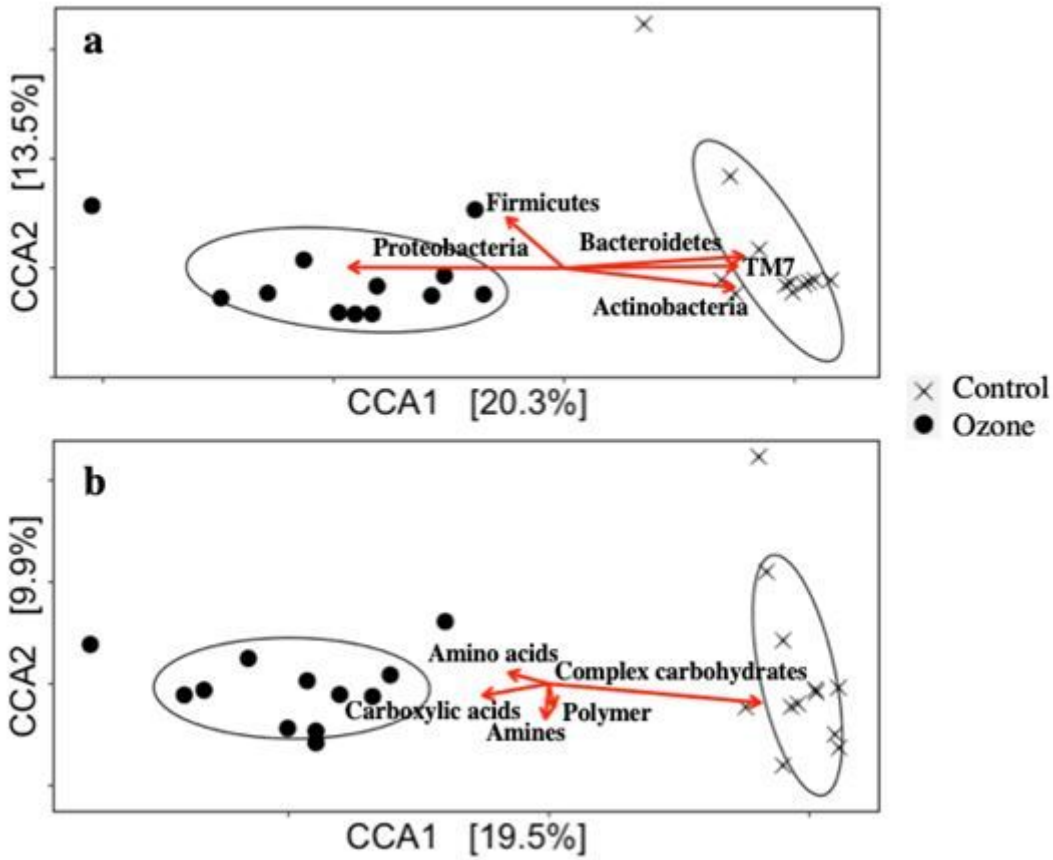


Figure 2

(a) CCA analysis of OTU composition with relative abundance of Actinobacteria, Proteobacteria, Firmicutes, Bacteroidetes and TM7 as constraining variable. (b) CCA analysis of OTU composition with metabolic rate of Amino acids, Carboxylic acids, Amines, Polymer and Complex carbohydrates as constraining variable

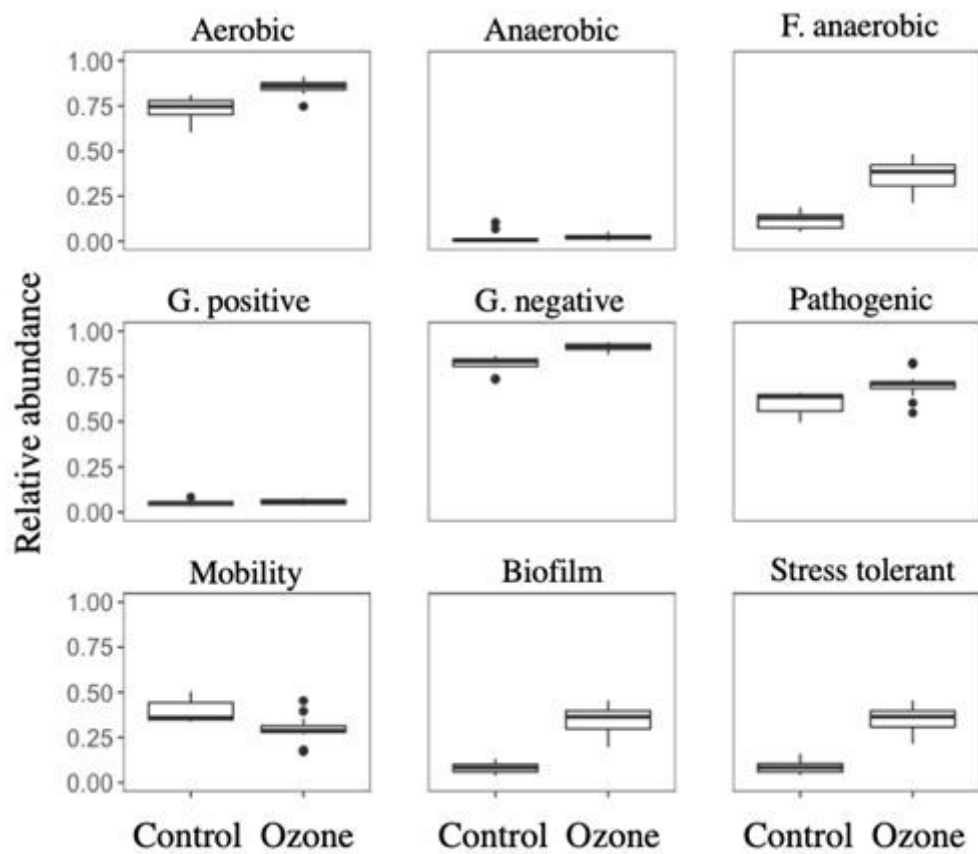


Figure 3

Community functional mapping using the Bugbase database, for quantifying relative abundance of traits in nine categories- Statistically differentiated Metacyc pathways predicted by PICRUST2 and filtered with ALDEx2 corrected Wilcoxon test.

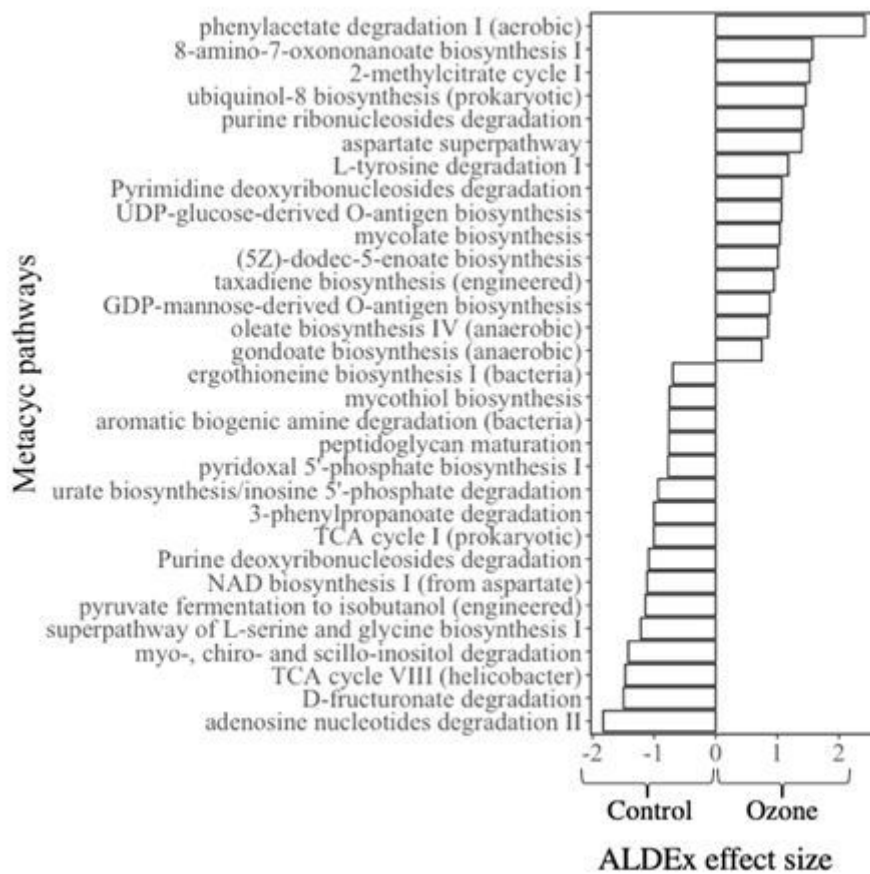


Figure 4

Statistically differentiated Metacyc pathways predicted by PICRUSt2 and filtered with ALDEx2 corrected Wilcoxon test.

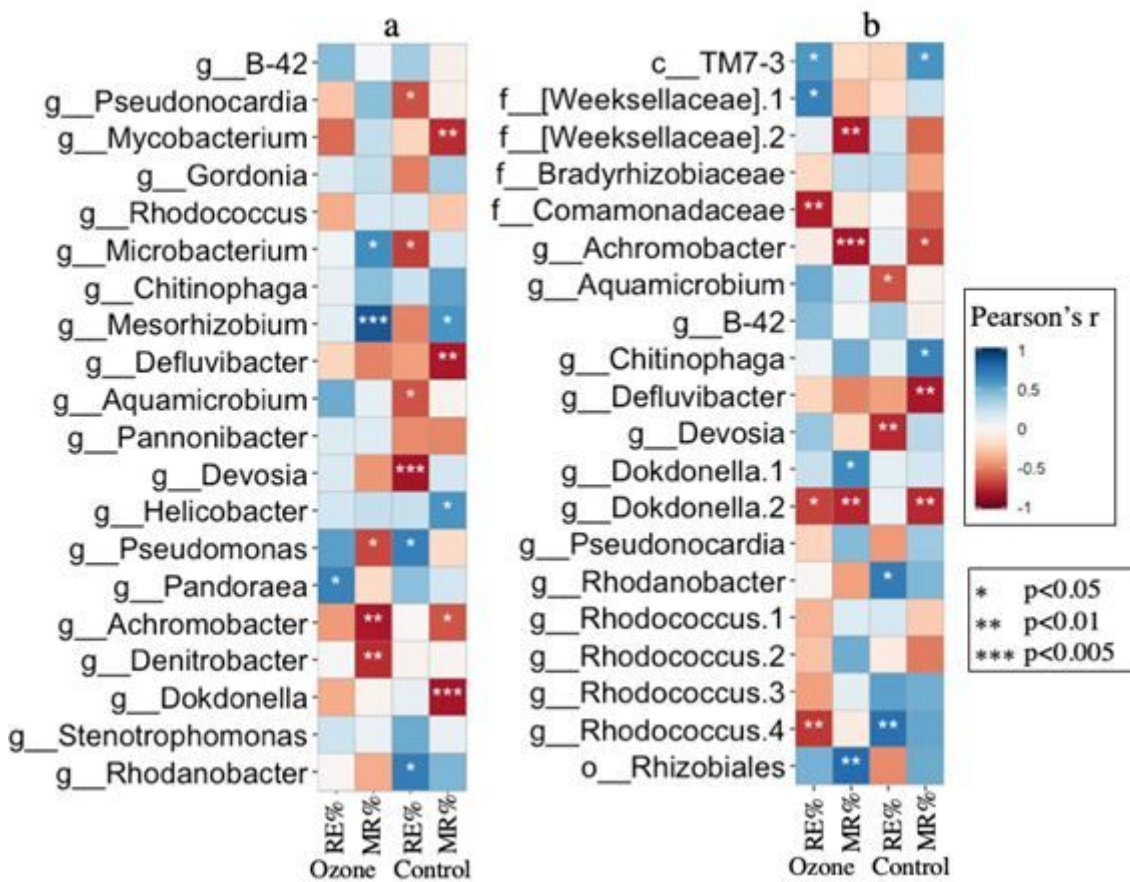


Figure 5

Top 20 taxa in average relative abundance in all samples, and their Pearson correlation with removal efficiency (RE%) and mineralization rate (MR%) in two biofilters. (a) Genus level. (b) OTU level, named for the lowest taxa rank identified with confidence over 97%, numbers are appended after names if different OTUs share the same lowest rank name.

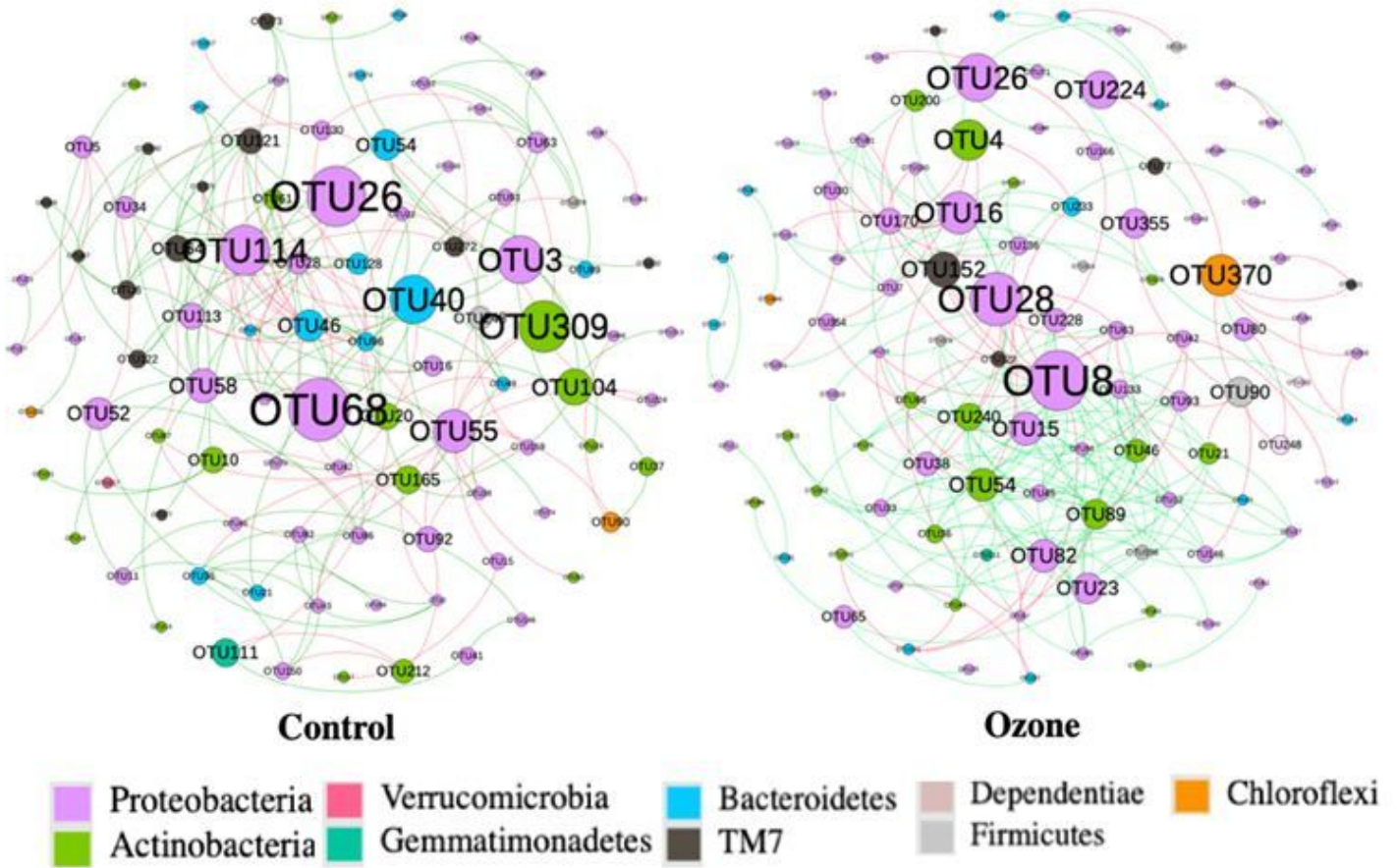


Figure 6

Microbial network in two biofilters with node color as Phylum, node size for betweenness and edge color as positive or negative correlations.

Supplementary Files

This is a list of supplementary files associated with this preprint. Click to download.

- [sup2.tsv](#)
- [sup1.xlsx](#)